V.A.4 Tailored High-Performance Low-PGM Alloy Cathode Catalysts

Vojislav R. Stamenkovic (Primary Contact) and Nenad M. Markovic

Argonne National Laboratory (ANL)
Argonne, IL 60439
Phone: (630) 252-8946
Email: vrstamenkovic@anl.gov

DOE Manager: Nancy L. Garland
Phone: (202) 586-5673
Email: Nancy.Garland@ee.doe.gov

Subcontractors:
- Karren More, Oak Ridge National Laboratory (ORNL) Oak Ridge, TN
- Peidong Yang, Lawrence Berkeley National Laboratory (LBNL), Berkeley, CA
- Rod Borup Los Alamos National Laboratory (LANL) Los Alamos, NM

Project Start Date: October 2015
Project End Date: September 2018

Overall Objectives

- Develop and deliver advanced low platinum group metal (PGM) cathode catalysts for use in polymer exchange membrane (PEM) fuel cells with increased mass activity at high electrode potentials, enhance performance at high current density.

- Improve durability while reducing the total loading of PGM and cost.

- Reduce PGM loading in the catalyst through alloying of Pt with other transition metals.

- The low-PGM materials will be in form of nanomaterials deployed on high surface area supports.

- Rational development and evaluation of durable high surface area supports for tailored nanomaterials.

- Development and implementation of scalable chemistry that would allow synthesis of tailored nanomaterials at the gram scale.

- Insight on the differences and similarities between the rotating disk electrode (RDE) and membrane electrode assembly (MEA) performance.

- Ionomer catalyst interaction and optimization of catalyst layers.

- The MEA will have a total PGM loading of <0.125 mg_{PGM}/cm^2 and 0.125 g_{PGM}/kW with mass activity higher than 0.44 A/mg_{PGM}.

- Total loss of electrochemically mass activity will be less than 40%.

Fiscal Year (FY) 2016 Objectives

- Development of active and durable catalysts for fuel cell cathodic reaction.

- Synthesis, structural and electrochemical evaluation of Pt-alloy nanoparticles with controlled physical parameters such as size, compositional profile and topmost surface.

- Development of scalable process to produce larger quantities of catalysts.

- Integration and evaluation of novel carbon supports with tailored Pt-alloy nanoparticles.

- Reproducibility of performance measured in MEA for tailored Pt-alloy catalysts with total PGM loading of <0.125 mg_{PGM}/cm^2 and mass activity over 0.44 A/mg_{PGM}.

Technical Barriers

This project addresses the following technical barriers from the Fuel Cells section 3.4.5 Technical Task Descriptions section of the Hydrogen, Fuel Cells and Infrastructure Technologies Program Multi-Year Research, Development, and Demonstration Plan.

(A) Durability: Develop improved catalysts

- Reduce precious metal loading of catalysts

- Increase the specific and mass activities of catalysts

- Increase the durability/stability of catalysts with cycling

- Test and characterize catalysts

Technical Targets

The project is aimed to develop nanoparticles with tailored architectures and composition based on Pt-alloys with transition metals PtM (M = Ni, Co, Cr, V, Ti, etc.), including alloys with Au, to improve performance for the fuel cell cathodic oxygen reduction reaction. The design principles will be focused to produce systems with low content of platinum group metals while exhibiting highly active and durable electrochemical properties evaluated in MEAs that will meet and/or exceed the DOE 2020 targets (Table 1).

TABLE 1. Progress Towards Meeting DOE 2020 Technical Targets for Electrocatalysts

	Unit	2015 DOE Targets	Project Status
PGM Total Loading	mg_{PGM}/cm^2	0.125	0.120
Mass Activity	A/mg_{Pt} @ 900 mV	0.44	0.60
Mass Activity Loss	%	<40	<20

FY 2016 Accomplishments

- Established three new labs at ANL as integral part of this project:

  - Development of an RDE coupled online with inductively coupled plasma mass spectrometry (ICP-MS) for detection of ultra-low concentration, part per trillion (ppt), of metals such as Pt, Au, Ni, Co, Fe, etc.

- Development of an MEA characterization test stand.

- Development of a laboratory for scaling the amounts of synthesized nanomaterials.

- Demonstrated capabilities of RDE ICP-MS setup by quantifying the amounts of dissolved Pt in a single potential cycle for different Pt surfaces, including Pt nanoparticles (NPs).

- Achieved detection limit of a micro monolayer of dissolved Pt.

- Evaluated benefits of subsurface Au in stabilization of Pt-based catalysts that completely diminished Pt dissolution.

- Developed highly active and durable multi-metallic system based on subsurface Au and PtNi over layer with Pt-skin surface.

- Evaluated transition from solid solution into intermetallic structure for Pt_3Co and PtCo by high-angle annular dark field (HAADF) and energy dispersive X-ray (EDX).

- Electrochemical characterization of PtCo catalysts with intermetallic structures.

- Identified Pt-skin surface in PtNi nanoframes as a descriptor for highly active and stable nanoframes by in situ extended X-ray absorption fine structure analysis (EXAFS).

- Synthesized novel nanoscale architectures in form of nanowires, nanoflowers, and highly porous Pt-alloy particles with promising catalytic properties.

- Established scalable chemistry to produce grams amount of PtNi catalyst with multilayered Pt-skin surfaces.

- Exceeded mass activity 2020 DOE Technical Targets for PtNi catalyst in MEA; mass activity = 0.6 A/mg_{Pt}.

✧　　✧　　✧　　✧　　✧

INTRODUCTION

The major obstacle for broad utilization of polymer electrolyte fuel cells (PEMFCs) in transportation is cost, performance, and durability of Pt catalysts that are employed in each individual cell of a fuel cell stack. Considering that Pt is the best known catalyst for both hydrogen oxidation reaction and oxygen reduction reaction (ORR), it is of paramount importance to develop a practical catalysts that will exhibit optimal performance through high specific activity (current per electrochemical surface area of catalyst), with minimal content of PGM that will ensure high mass activity (current per mass unit of PGM). Cathodes in PEMFCs suffer from substantial kinetic limitations and degradation of catalysts for ORR; and for that reason, the main focus in catalyst development is to create highly efficient, durable cathodes with low content of PGM. Therefore, this project will aim to develop and deliver advanced, low-PGM cathode catalysts for PEMFC that will increase mass activity at high electrode potentials, enhance performance at high current density, and improve durability while decreasing the cost. The decrease of the total loading of PGM in the fuel cell will be accomplished by improving activity and durability of Pt-based catalysts through alloying with other transition metals [1]. These PGMs in the form of nanomaterials will be deployed on high surface area supports in the cathode of MEA with total PGM loading less than the DOE 2020 target of 0.125 mg_{PGM}/cm^2 and 0.125 mg_{PGM}/kW with mass activity higher than 0.44 A/mg_{PGM}.

APPROACH

This is a multi-performer project led by ANL supported by inter-laboratory collaborations with LBNL, LANL, and ORNL. ANL will lead and coordinate this applied research effort with other national laboratories; will define project scope, topics, and milestones; and will be responsible for deliverables as well as quarterly and annual reports to Fuel Cell Technologies Office. LBNL will be involved in chemical synthesis of advanced nanoscale structures and development of scaling-up protocols of the most promising catalytic systems. LANL will execute fabrication and testing of the MEA and will provide alternative carbon based supports to conventional high surface area carbon. ORNL will perform electron microscopy characterization of synthesized materials and catalyst deployed in MEA before and after testing protocols. The approach of this project is based on the knowledge obtained from well-defined systems that will be used to tailor functional properties of corresponding nanoscale materials, with desired shape, size, structure and compositional profile. Integration of engineered nanomaterials in electrochemical systems requires integration of a broad range of scientific disciplines such as

solid state physics, surface science, physical chemistry, and electrochemistry. This effort also includes the combination of highly diverse experimental tools supported by state-of-the-art synthesis and characterization strategies, together with the fabrication and testing capabilities. The project is executed *simultaneously* in five tasks throughout duration of the project: Task 1 well-defined systems, Task 2 synthesis of nanoscale materials, Task 3 electrochemical and structural characterization of catalysts, Task 4 supporting materials for novel catalysts, and Task 5 scaling up of catalysts.

RESULTS

Insight into Pt Dissolution by RDE ICP-MS. In addition to development of novel catalytically active materials for fuel cells, it is of paramount importance to get detailed insight into fundamental properties related to their stability in an electrochemical environment. An analytical

setup was developed for characterization of catalyst in the form of single crystals, thin films, and nanoparticles by coupling RDE with ICP-MS, see schematic illustration in Figure 1. This setup has achieved an ultimate sensitivity that was verified first on the extended single crystalline surfaces of Pt electrodes [2]. In these experiments it was possible to detect and measure the amount Pt dissolved in a single potential cycle. The range of dissolved Pt varies depending on crystallographic orientation and it was found to increase with the decrease of Pt coordination number. The most stable surface was Pt(111), while the least stable was Pt(110). The amounts of dissolved Pt ranged from 2–83 µML (mono atomic layer) in a single potential cycle for Pt(111) and Pt(110) respectively. For fuel cell applications, the most relevant finding was the amount of dissolved Pt in a single potential cycle from Pt/C catalyst, which was found to be around 103 µML per cycle in the case of Pt/C TKK particles with mean diameter of 3 nm, as shown in Figure 1a. It would also
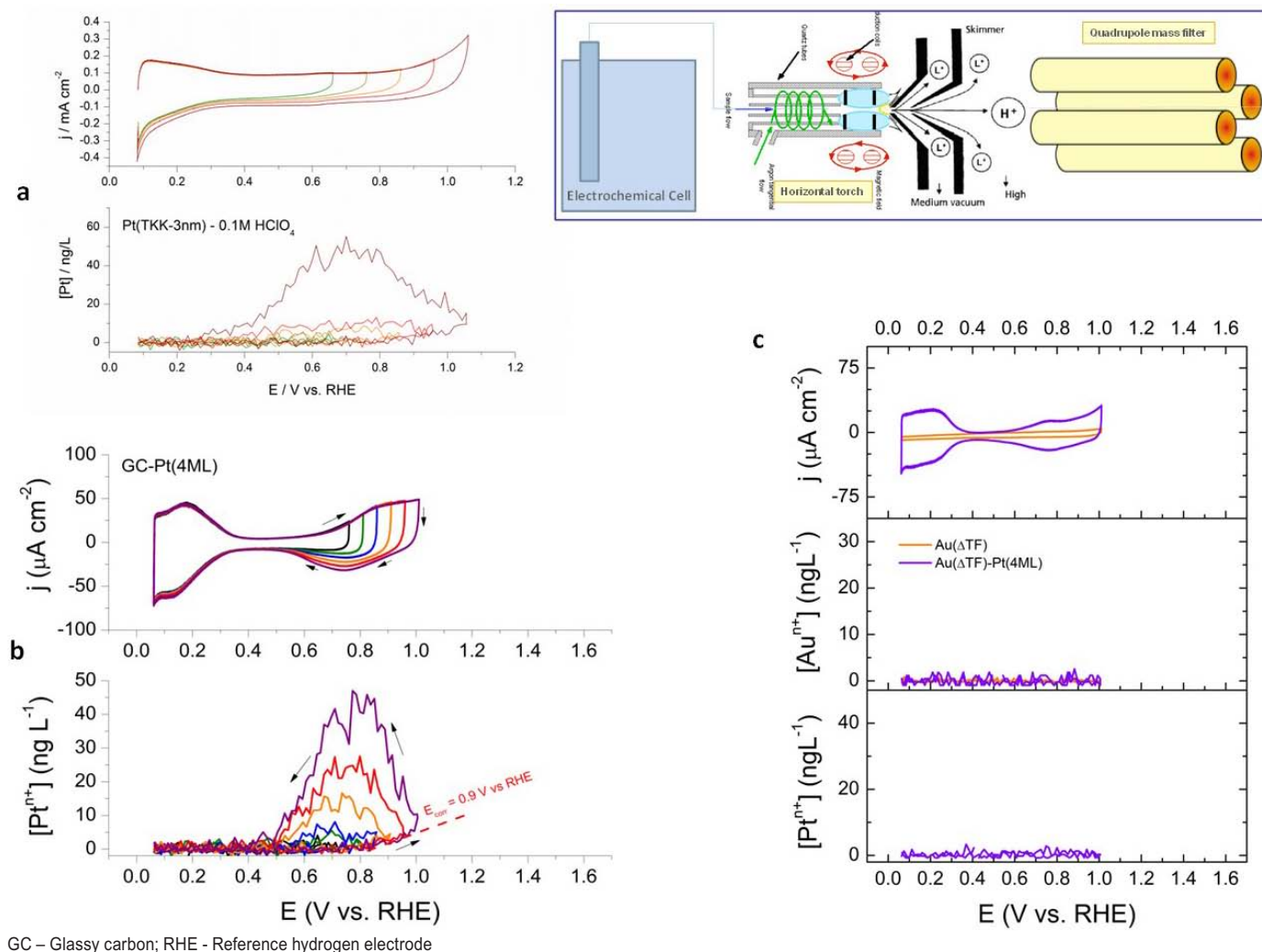

GC – Glassy carbon; RHE - Reference hydrogen electrode

FIGURE 1. Schematic illustration of RDE ICP-MS method and cyclic voltammetry with corresponding Pt dissolution curve in 0.1 M HClO$_4$. (a) Pt/C TKK-3 nm catalyst. (b) 4 atomic monolayer thick Pt thin film on glassy carbon electrode. (c) 4 atomic monolayer thick Pt thin film over Au subsurface deposited on glassy carbon electrode.

be important to mention, that RDE ICP-MS setup developed in our labs is capable to distinguish two events, dissolution of Pt vs. detachment of particle from the substrate. For that reason, the measured amount of dissolved Pt has not been assigned to detached Pt particles. Considering our previous reports on the beneficial role of subsurface Au [3,4] and the fact that these values are closely tied to Pt fundamental properties as well as, it was intriguing to evaluate Pt systems with Au substrate and check by RDE ICP-MS whether addition of the metal that is less oxophilic affects dissolution of Pt. For that purpose we have done a series of experiments with well-defined thin films' compositional profiles, with and without Au substrate. It has been found that addition of Au as a substrate can dramatically affect the amount of dissolved Pt. Figure 1b and 1c shows the results measured on a glassy carbon electrode covered only with 4 ML of Pt, and the same amount, 4 ML thick topmost Pt layer that was deposited over Au substrate in the form of thin film. While Pt dissolution from 4 ML Pt thin film is severe, glassy carbon electrode covered first with Au substrate does not exhibit any signal for dissolved Pt. This is rather strong proof that subsurface Au can play a major role in hindering Pt dissolution. This finding will serve as foundation for the follow up studies related to the optimization of parameters such as thickness of the Au substrate as well as Pt over layer, including associated annealing conditions. This approach is expected to evolve towards more complex systems which would allow identification of the most desirable composition in terms of minimal amount of precious metals and high catalytic activity for the ORR.

Atomic Structure of Pt$_3$Ni Nanoframe Electrocatalysts by In Situ X-ray Absorption Spectroscopy. The success rate in synthesis and quality of the nanoframe catalyst has been evaluated by in situ X-ray absorption near-edge spectroscopy (XANES) and EXAFS measurements to address the difference in performance among lab scale batches that were verified by both RDE and MEA [5]. The surface characteristics of the nanoframes were probed through electrochemical hydrogen underpotential deposition and carbon monoxide electro-oxidation, which showed that nanoframe surfaces with different structure exhibit varying levels of binding strength to adsorbate molecules. In our previous work we have shown that Pt-skin formation on Pt-Ni catalysts will enhance ORR activity by weakening the binding energy between the surface and adsorbates [6,7]. Ex situ and in situ XAS results reveal that nanoframes which bind adsorbates more strongly have a rougher Pt surface caused by insufficient segregation of Pt to the surface and consequent Ni dissolution. In contrast, nanoframes which exhibit rather high ORR activity simultaneously demonstrate more significant segregation of Pt over Ni-rich subsurface layers, allowing better formation of the critical Pt-skin. In situ XAS analyses performed with the working electrode that was cycled to condition the catalyst and then held at 0.9 V vs. RHE for in situ ORR, yields a clear picture of the differences

in atomic distribution and structuring in Pt$_3$Ni(1.0) and Pt$_3$Ni(1.5), where 1.0 and 1.5 reflect the ratio between integrated charges obtained from the H$_{upd}$ and CO stripping curves. From the XANES spectra in Figure 2a at the Ni K-edge and Pt L_3-edge, the decrease in white line intensity indicates surface NiO dissolution in the acidic electrolyte after potential cycling. It was also found that at both metal edges, the XANES spectra were identical, and therefore, the oxidation states of both metals in both samples were deemed identical (Figures 2a–2b). The near-edge region of X-ray absorption probes electronic transitions from a core level into local, unoccupied states just above the Fermi level energy. During in situ ORR, the Fermi levels of the Pt$_3$Ni metallic samples are controlled by the potentiostat at an identical potential relative to a reference electrode potential. Therefore, the probability of an X-ray absorption-induced transition into the unoccupied states is similar for these samples while under potential control, and their XANES spectra are identical. However, as can be seen from Figures 2c–2d, after removing the electrode from the electrolyte and rinsing and drying it, the XANES spectra are no longer identical between Pt$_3$Ni(1.0) and Pt$_3$Ni(1.5). The Ni in Pt$_3$Ni(1.0) is more oxidized while the Pt is more reduced, indicating increased donation of electron density from Ni to Pt in Pt$_3$Ni(1.0). The increased alloying in Pt$_3$Ni(1.0) was further supported by the EXAFS analysis. Figure 2e shows a XANES difference spectrum at the Ni K-edge for Pt$_3$Ni(1.0) and Pt$_3$Ni(1.5) samples where the normalized absorption in situ is subtracted from the normalized absorption after ORR. After the catalyst is rinsed and dried under nitrogen, the nickel in Pt$_3$Ni(1.0) is more easily oxidized as indicated by the more intense peak at the white line position, approximately 16–17 eV after the edge. The platinum shell is not protecting the nickel as thoroughly in Pt$_3$Ni(1.0), suggesting the surface has more low coordination sites and a thinner platinum shell, as illustrated in Figure 2f. These conclusions were further substantiated by EXAFS data. The initial observation in the first shell fit is that the total coordination numbers N_{Pt} and N_{Ni} are similar for both samples, with N_{Pt} significantly smaller than N_{Ni}. As mentioned, this indicates that Pt atoms have segregated to the surface to form some variation of the desired Pt-skin structure because of the lower coordination number of surface atoms. It was also found that the heterometallic coordination of nickel to platinum is decreased in Pt$_3$Ni(1.5), and correspondingly the homometallic coordination is increased. This depicts the nanoframe of Pt$_3$Ni(1.5) as one with more segregation of Pt from Ni, which is also indicated by the smaller extent of alloying parameters for platinum, J_{Pt}, calculated for Pt$_3$Ni(1.5) vs. Pt$_3$Ni(1.0). In situ EXAFS demonstrated that Pt$_3$Ni(1.0) had a larger extent of alloying while Pt$_3$Ni(1.5) had more significant segregation of Pt to the surface of the nanoframe. It was concluded that Pt$_3$Ni(1.0) has a thinner, rougher Pt surface caused by insufficient segregation of Pt to the surface. Pt$_3$Ni(1.5) exhibits extremely high ORR activity due to its significant segregation of Pt
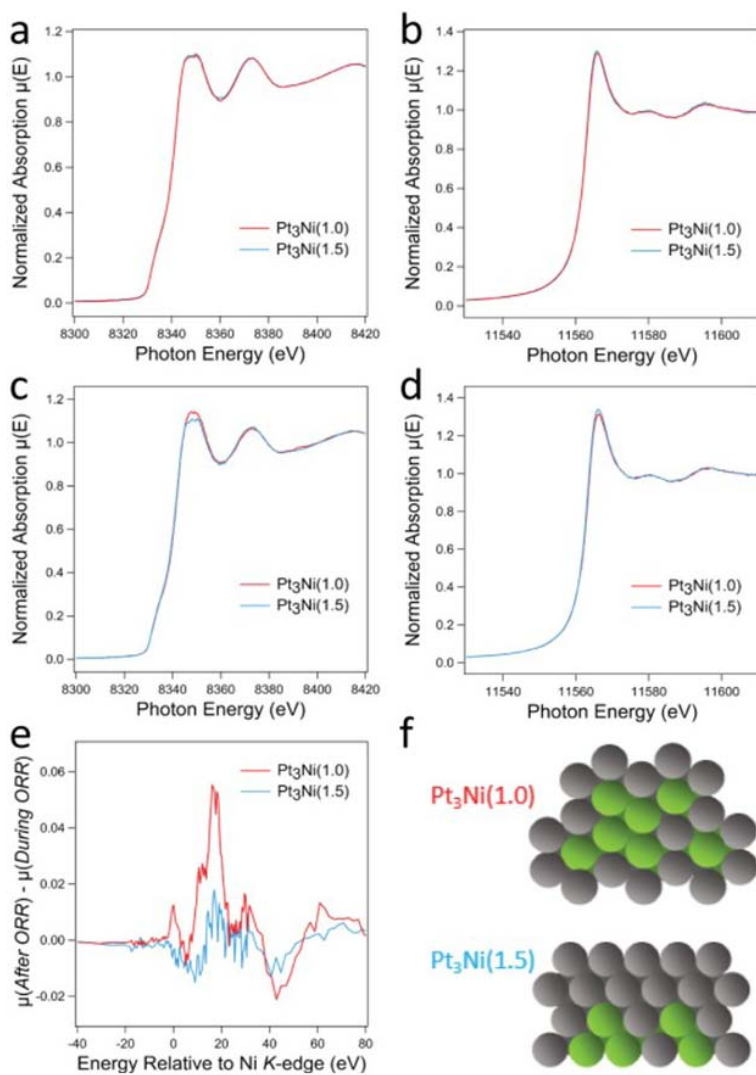
FIGURE 2. XANES of Pt$_3$Ni/C catalysts in situ and after electrochemistry. (a) Ni *K*-edge at 0.9 V. (b) Pt *L3*-edge at 0.9 V. (c) Ni *K*-edge after in situ. (d) Pt *L3*-edge after in situ. (e) Ni *K*-edge in situ XANES subtracted from after in situ XANES. (f) Model surfaces of Pt$_3$Ni(1.0) and Pt$_3$Ni(1.5), where gray atoms are Pt and green atoms are Ni. With permission from the American Chemical Society [5].

elemental surface rearrangement upon thermal annealing from room temperature (RT) to 800°C: (1) random elemental distribution; (2) surface skin-layer formation; (3) ordered domain nucleation; (4) ordered framework development; and (5) amorphization. A comprehensive interplay among phase evolution, surface faceting, and elemental inter-diffusion is revealed. No obvious faceting was observed on the initial NP surface at RT. Increasing the temperature to 350°C results in Pt segregation to the surface region, as evidenced by a slightly brighter contrast on the particle surface compared to that at RT (Figure 3a). Pt segregation can be clearly demonstrated from an image intensity profile taken across the diameter of the NP, where the intensity measurement of the contrast associated with the atomic columns shows an obvious increase in contrast at the surface region, which is consistent with segregation of Pt atoms to the surface. Similar Pt surface segregation behavior was observed for other Pt$_3$Co NPs on the same sample; this is consistent with results from some earlier studies of Pt$_3$Ni NPs [1,]. Furthermore, the surface facets appear to sharpen at 350°C compared to those observed at RT, where {1-10} and {110} facets are clearly observed (marked by arrow in Figure 3a). Surface faceting is likely a combined result of Pt segregation to the surface and the initiation of atomic surface reconstruction during the early stage of annealing, which is consistent with earlier studies. It is important to note that such Pt-enriched surfaces disappear once the annealing temperature is increased to 550°C. Hence, the results show that the formation of a Pt-segregated surface over as-synthesized Pt$_3$Co NPs is sensitive to the annealing temperature. Such sensitivity can be explained by the interplay between surface segregation and compositional disordering. The segregation process of Pt to the NP surface (with disordered Pt and Co elemental atoms) is mainly driven by the decrease in free energy owing to negative surface segregation enthalpy. Such segregation will lead to a decrease in configurational entropy of the system by inducing surface compositional ordering. While surface-segregation free energy eventually turns positive due to the increased entropic contribution, increasing annealing temperature, therefore, results in the observed disappearance of the Pt-segregated surface. Such surface diffusion of Pt was also confirmed by energy dispersive X-ray spectroscopy (EDS) chemical mapping in other particles at different annealing temperatures. The Pt$_3$Co nanoparticle originally attains a homogenous elemental distribution at RT. Pt enrichment could be seen when the particle was heated to 350°C, but it vanished when the temperature was increased

from Ni, allowing for better formation of a Pt-skin [5]. The activity of a given nanoframe sample was resolved to be primarily predetermined by the level of platinum enrichment at the edges of the rhombic dodecahedron, which altogether represents important guidelines for successful synthesis of highly active PtNi nanoframes.

Evolution of Surface Faceting and Elemental Diffusion at the Atomic-level for Pt$_3$Co Nanocatalysts. In situ high temperature annealing in an aberration-corrected scanning transmission electron microscope (STEM) was performed to discern the thermally driven structural and compositional evolution of individual Pt-Co alloy NPs [8]. It was found that Pt$_3$Co nanoparticles undergo five distinct stages of
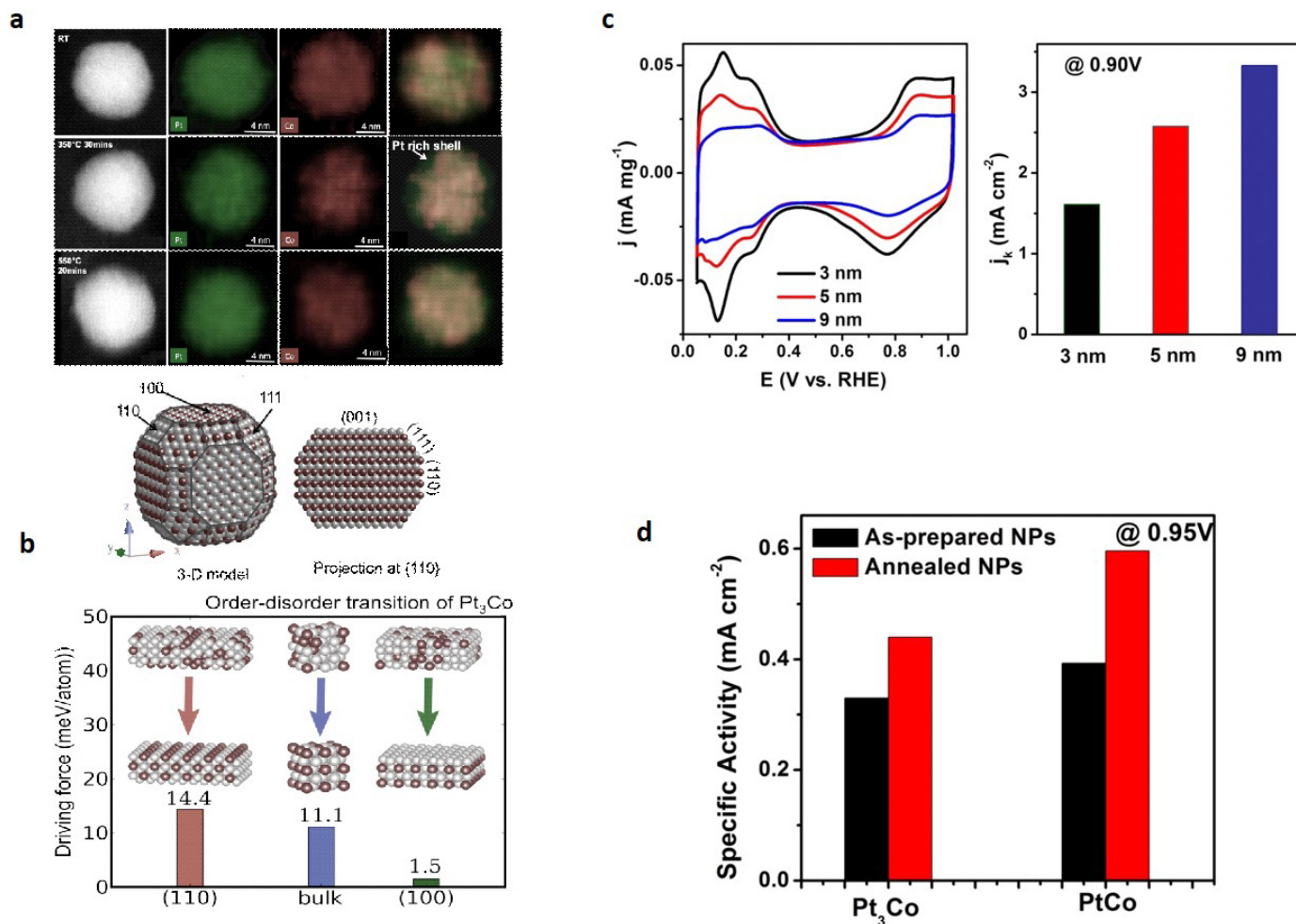
FIGURE 3. Evolution of surface faceting and elemental diffusion at the atomic-level for Pt$_3$Co nanoparticle during thermal annealing and corresponding electrochemical properties. (a) HAADF images and corresponding EDS elemental maps of a Pt$_3$Co nanoparticle which was annealed at different temperatures: RT, 350°C, and 550°C respectively. The overlapped maps of Co and Pt (shown in the last column) demonstrate that Pt segregates to the particle surface at 350°C and diminishes at the surface when it is annealed at 550°C. (b) Detailed geometry correspondence between the facets and the two dimensional projection down [110] and the driving forces to form ordered structure at different facets and bulk by using first-principles density functional theory, showing that [110] has the highest driving force to form ordered structure. (c, d) Cyclic voltammetry of intermetallic Pt$_3$Co NPs along with the ORR bar graphs that show particle size dependence and electrochemical performance at both 0.9 V and 0.95 V. With permission from the Nature publishing group [8].
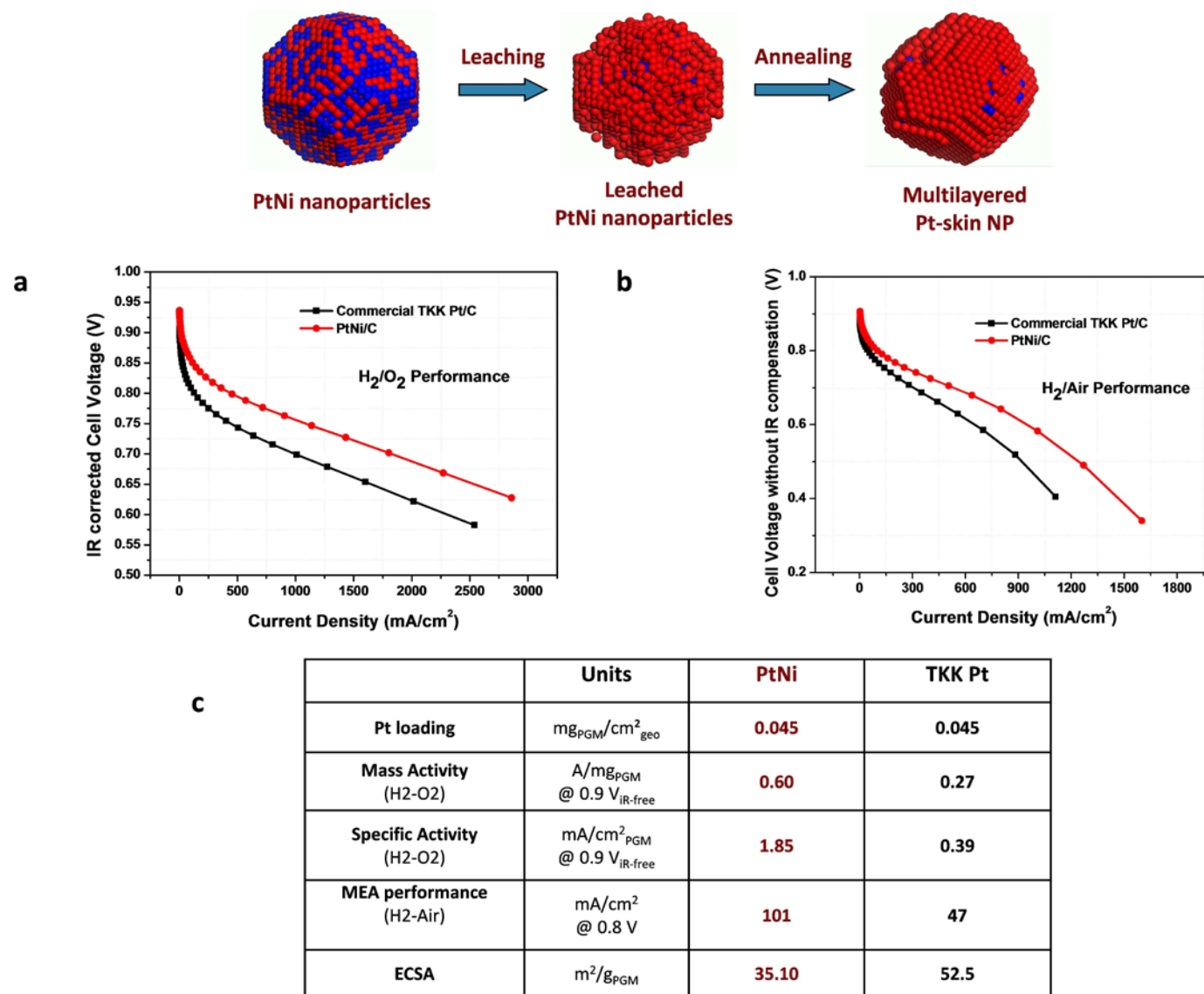
further to 550°C. Our results suggest that careful selection of annealing temperature is indispensable in order to form Pt-segregated surface architecture for enhanced catalytic activity. Moreover, the ordered structures on the (1–10) surface propagated throughout the {001} planes to the [-110] planes with further annealing at 600°C (Figures 3a and 3b). When the particle was annealed at 600°C for a longer time, elemental inter-diffusion into the bulk increased as evidenced by the largely inhomogeneous intensity distribution. The ordering structure on two sides, i.e., those close to {001} surfaces, eventually formed with a further annealing at 600°C, resulting in a completely ordered structure. This phase transformation is consistently characterized by the distinct Pt$_3$Co NPs under these annealing conditions. Continued annealing at 600°C for 20 min does not change the

ordering architecture but leads to further elemental inter-diffusion. No noticeable elemental diffusion or structure change was observed with further annealing at 700°C for 30 min, which suggests that the particle has reached a thermally stable state with an L1$_2$ structure. Our observation on the evolution of the ordering structure shows that the ordered framework was established first in the NPs followed by additional diffusion to a stable ordered structure. When the particle is further annealed at 800°C, the atomic columns in the HAADF image were blurred resulting from increased atomic vibration at the elevated temperature, although the ordering structure is still vaguely visible. Longer annealing times at 800°C activate the amorphization (i.e., pre-melting) of the nanoparticle and the morphology eventually takes on a rounded shape. Electrochemical characterization shown

in Figures 3c and 3d depicts noticeable improvement in catalytic properties of the ORR for both Pt₃Co and PtCo NPs. Influence of ordered phase in Pt-alloys on electrochemical durability will be explored in future.

MEA Evaluation of PtNi/C with Multilayered Pt-skin Surfaces. The NP evaluations were made in RDE and 5 cm² MEA at ANL. The MEAs were made by the decal method with the ionomer and membrane in the proton form and hot-pressing of the decals to the membrane at 130°C. The ionomer to carbon ratio was 0.8. The summary of the MEA test results is given in Figure 4. The MEAs were tested temperatures ranging from room temperature to

80°C, with 150 kPa(abs) humidified hydrogen on the anode at 1 L/min, and with 150 kPa(abs) humidified oxygen and/ or air on the cathode, with a relative humidity of 100%. The mass activities are shown in the table of Figure 4c. High performance PtNi or multilayered Pt-skin NPs have been evaluated by MEA and it has been confirmed that high durability originates from the protective multilayered Pt-skin surface that encapsulates core that is Ni rich, as mentioned before. The multilayered Pt-skin catalyst was prepared from colloidal PtNi NPs (~5 nm) by following the recent report from our group (more details about synthesis will be given in the next section). In the previous quarter we have achieved DOE 2020 Technical Target, while in this quarter, mass

	Units	PtNi	TKK Pt
Pt loading	mg$_{PGM}$/cm²$_{geo}$	0.045	0.045
Mass Activity (H2-O2)	A/mg$_{PGM}$ @ 0.9 V$_{iR-free}$	0.60	0.27
Specific Activity (H2-O2)	mA/cm²$_{PGM}$ @ 0.9 V$_{iR-free}$	1.85	0.39
MEA performance (H2-Air)	mA/cm² @ 0.8 V	101	47
ECSA	m²/g$_{PGM}$	35.10	52.5

ECSA – Electrochemically active surface area

FIGURE 4. Electrochemical evaluation of ~20 wt% PtNi/C with multilayered Pt-skin surfaces (red) and Pt/C TKK (black) obtained by 5 cm² MEA. (a) Hydrogen–oxygen polarization curves. (b) hydrogen–air polarization curves. The cathode Pt loading is 0.046 mg$_{Pt}$/cm², ionomer to catalyst = 1, 80°C, 150 kPa, 100% relative humidity. (c) Performance parameters of PtNi/C retrieved from MEA hydrogen–oxygen polarization curves.

activity over-achieved the DOE target even though the Pt loading on cathode was substantially decreased to the value of 0.045 mg_{PGM}/cm^2. Measured mass activity was found to be 0.60 A/mg_{PGM} at 0.9 V. Achieved mass activity combined with the catalyst loading indicates that the project milestone has been met.

CONCLUSIONS AND FUTURE DIRECTIONS

- Evaluation of activity, durability, and optimization of MEA protocols at ANL and LANL.

- Alternative approaches towards highly active and stable catalysts with low PGM content.

- Tailoring of the structure and composition that can optimize durability and performance in Pt-alloys.

- Synthesis of tailored low-PGM practical catalysts with alternative supports.

- Structural characterization (in situ XAS, high resolution transmission electron microscopy, X-ray diffraction).

- Resolving the surface chemistry in MEAs through electrochemical evaluation in RDE and MEA.

- In situ durability studies for novel catalyst-support structures (RDE ICP-MS).

- Scale-up of chemical processes to produce gram quantities of the most promising catalysts.

SPECIAL RECOGNITIONS & AWARDS/ PATENTS ISSUED

1. V.R. Stamenkovic, C. Wang, N.M. Markovic, *Bimetallic Alloy Electrocatalysts with Multilayered Platinum Skin Surfaces*, United States Patent; US 9,246,177 B2, Jan. 26, 2016.

2. C. Chen, Y. Kang, N.M. Markovic, G. Somorjai, Peidong Yang and V.R. Stamenkovic, Patent Pending *Highly Crystalline Pt₃Ni Nanoframes with Three-Dimensional Electrocatalytic Surfaces*.

FY 2016 PUBLICATIONS/PRESENTATIONS

1. H. Lv, D. Li, D. Strmcnik, A.P. Paulikas, N.M. Markovic, V.R. Stamenkovic, *The design of tailored nanomaterials for efficient oxygen reduction reaction,* DOI:10.1016/j.nanoen.2016.04.008, **Nano Energy (2016)**.

2. D. Li, H. Lv, Y. Kang, N.M. Markovic, and V.R. Stamenkovic, *Recent Advances in the Development of Oxygen Reduction Reaction Catalysts for Low Temperature Fuel Cells,* DOI: 10.1146/annurev-chembioeng-080615-034526, **Annual Review of Chemical and Biomolecular Engineering**, Vol. 7 (2016).

3. P.P. Lopes, D. Strmcnik, J. Connell, V.R. Stamenkovic and N.M. Markovic, *Relationships between Atomic Level Surface Structure and Stability/Activity of Platinum Surface Atoms in Aqueous Environments,* **ACS Catalysis**, 6 (4), 2536-2544, 2016.

4. D. Li, D. Strmcnik, N. Markovic and V. Stamenkovic, *(Invited Lecture)Progress in Material Design of Electrocatalysts for Fuel Cells,* **2016 Materials Research Society Spring Meeting**, 2016, Phoenix, AZ,

5. D. Li, Y. Kang, J. Snyder, D. Strmcnik, N. Markovic and V. Stamenkovic *(Invited Lecture) Electrocatalysts with Advanced Properties,* **2015 Materials Research Society Fall Meeting**, 2015, Boston, MA.

6. D. Li, D. Strmcnik, N.Markovic and V. Stamenkovic (*Key Note Lecture*) *Advanced Catalysts with Ultra-Low PGM Content for PEMFC Cathode,* **The 2015 Electrolysis and Fuel Cells Discussions**, 2015, La Grande Motte, France.

7. N. Becknell, Y. Kang, Chen Chen, J. Resasco, N. Kornienko, J. Guo, N.M. Markovic, G.A. Somorjai, V.R. Stamenkovic, P. Yang, *Atomic Structure of Pt₃Ni Nanoframe Electrocatalysts by in Situ X-ray Absorption Spectroscopy,* **Journal of American Chemical Society**, 137 (2015) 15817.

8. V. Stamenkovic, N. Markovic, D. Strmcnik, D. Li., Y. Kang, *(Plenary Lecture) From Well-Defined Interfaces to Functional Nanoscale Materials,* **The 7th International Fuel Cells Workshop**, 2015, Kofu, Japan.

9. M. Chi, C. Wang, Y. Lei, G. Wang, K.L. More, F. Allard, N.M. Markovic, and V.R. Stamenkovic, *Surface faceting and elemental diffusion behaviour at atomic scale for alloy nanoparticles during in situ annealing*, **Nature Communications**, 6 (2015) *No.* 8925.

REFERENCES

1. V. Stamenkovic, B. Fowler, B.S. Mun, G. Wang, P.N. Ross, C. Lucas, and N.M. Markovic, "Improved Oxygen Reduction Activity on Pt₃Ni(111) via Increased Surface Site Availability," *Science.*, 315 (2007) 493–497.

2. P.P. Lopes, D. Strmcnik, J. Connell, V.R. Stamenkovic and N.M. Markovic, "Relationships between Atomic Level Surface Structure and Stability/Activity of Platinum Surface Atoms in Aqueous Environments," *ACS Catalysis*, 6 (4), 2536–2544, 2016.

3. C. Wang, D. van derVliet, K.L. More, N.J. Zaluzec, S. Peng, S. Sun, H. Daimon, G. Wang, J. Greeley, J. Pearson, A.P. Paulikas, G. Karapetrov, D. Strmcnik, N.M. Markovic, V.R. Stamenkovic, "Multimetallic Au/FePt₃ Nanoparticles as Highly Durable Electrocatalysts," *Nano Letters*, 11 (2011) 919–928.

4. Y. Kang, J. Snyder, D. Li, K. More, N.M. Markovic and V.R. Stamenkovic, "Multimetallic Core/Interlayer/Shell Nanostructures as Advanced Electrocatalysts," *Nano Letters*, 14 (2014) 6361–6367.

5. N. Becknell, Y. Kang, Chen Chen, J. Resasco, N. Kornienko, J. Guo, N.M. Markovic, G.A. Somorjai, V.R. Stamenkovic, P. Yang, "Atomic Structure of Pt₃Ni Nanoframe Electrocatalysts by in Situ X-ray Absorption Spectroscopy," *Journal of American Chemical Society*, 137 (2015) 15817.

6. C. Chen, Y. Kang, J. Snyder, M. Mavrikakis, Y. Li, N.M. Markovic, G. Somorjai, Peidong Yang, V.R. Stamenkovic, "*Highly Crystalline Multimetallic Nanoframes with Three-Dimensional Electrocatalytic Surfaces,*" Science, 343(2014)1339–1343.

7. C. Wang, M. Chi, D. Li, D. Strmcnik, D. van derVliet, G. Wang, V. Komanicky, K-C. Chang, A.P. Paulikas, D. Tripkovic, J. Pearson, K.L. More, N.M. Markovic and V.R. Stamenkovic, "Design and Synthesis of Bimetallic Electrocatalyst with Multilayered Pt-Skin Surfaces," *Journal of American Chemical Society*, **133** (2011)14396.

8. M. Chi, C. Wang, Y. Lei, G. Wang, K.L. More, F. Allard, N.M. Markovic, and V.R. Stamenkovic "Surface faceting and elemental diffusion behaviour at atomic scale for alloy nanoparticles during in situ annealing," *Nature Communications*, 6 (2015) *No.* 8925.